Chapter 8
Applications of Carbonation Technologies

Abstract Reduction of CO_2 emission in industries and/or power plants should be a portfolio option; for example, CO_2 capture and alkaline solid waste treatment can be combined through an integrated approach, i.e., accelerated carbonation. Gaseous CO_2 is fixed as thermodynamically stable solid precipitates, which are rarely released after mineralization. In addition, the proximity between the industrial CO_2 emission and the waste residue sources reduces transportation costs. This chapter presents an integrated approach (i.e., accelerated carbonation technology) to capturing CO_2 while improving the physico-chemical properties of alkaline solid wastes for the utilization in civil engineering. The carbonation of industrial alkaline wastes, such as steel slags and metalworking wastewater, has been proved to be an effective way to capture CO_2.

8.1 Concept of Accelerated Carbonation

The concept behind carbonation reaction is similar to natural weathering processes, where CO_2 reacts with metal oxide-bearing materials, such as CaO and MgO, to form stable and insoluble carbonates (such as $CaCO_3$ and $MgCO_3$). In this section, different types of carbonation technologies are first reviewed and discussed. The concept of the system mass and energy balance is then provided. Several key performance indicators for carbonation reaction are also illustrated.

8.1.1 Types of Carbonation Technologies

Figure 8.1 shows various approaches to integrating solid waste treatment with CO_2 fixation and utilization, including the following:

- Indirect carbonation (using natural ore or alkaline solid wastes)
- Direct carbonation (using natural ore or alkaline solid wastes)
- Carbonation curing (for the production of cement mortar or concrete block)

P.-C. Chiang and S.-Y. Pan, *Carbon Dioxide Mineralization and Utilization*, DOI 10.1007/978-981-10-3268-4_8

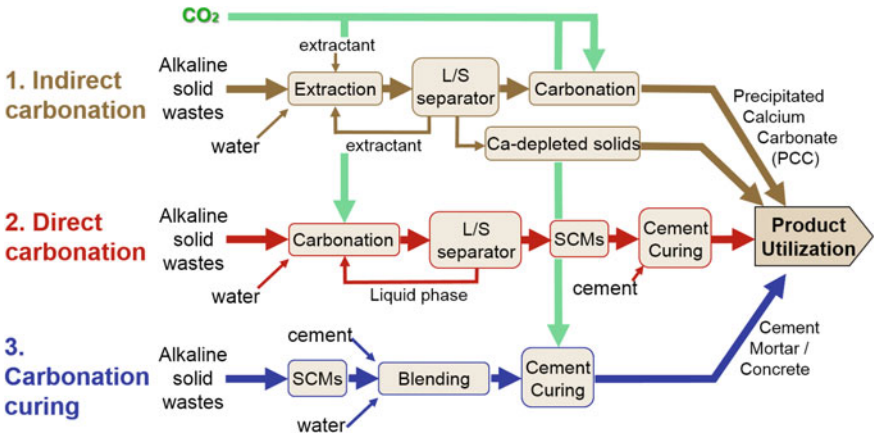

Fig. 8.1 Various approaches to integrating alkaline solid waste treatment with CO_2 fixation and utilization through carbonation process

For the indirect carbonation using alkaline solid wastes, high purity of $CaCO_3$ precipitates (e.g., 99%) can be produced and implemented as high value industrial materials, such as coating pigments and filters [1–3]. In contrast, the direct carbonation can fix CO_2 into carbonate precipitates with alkaline solid wastes, which is superior in providing high storage capacity and long storage time [4–6]. Another approach to integrating CO_2 with alkaline solid wastes treatment is the carbonation curing for blended cement or concrete through the injection of pressurized CO_2 gas (normally using pure CO_2 stream) into a sealed chamber.

8.1.2 System Mass and Energy Balance

The CO_2 mass balance can be carried out in the system by measuring the CO_2 loss in the gas phase as well as the increase of inorganic carbon content in both the liquid (i.e., total inorganic carbon (TIC) concentration) and solid phases (i.e., $CaCO_3$ content). Figure 8.2 shows the systematic diagram among gas, liquid, and solid phases.

Accordingly, the CO_2 mass balance equation can be developed as shown in Eq. (8.1):

$$\rho_{CO_2,i} Q_{g,i} C_{g,i} - \rho_{CO_2,o} Q_{g,o} C_{g,o} = Q_l \Delta C_{TIC} + Q_{sl} C_{s,act} (S/L) \tag{8.1}$$

where ρ_g (i.e., 1.796 g L^{-1}) is the density of CO_2 at standard temperature and pressure (STP); ΔC_{TIC} (g/L) is the concentration difference of the TIC in the liquid agents before and after carbonation; Q_l (L/min) is the liquid flow rate; Q_s (L/min) is the solid input rate; $C_{s,act}$ (g) is the mass of CO_2 captured in the solid waste; and L/S (mL/g) is the liquid-to-solid ratio. The molar volume of CO_2 is generally assumed

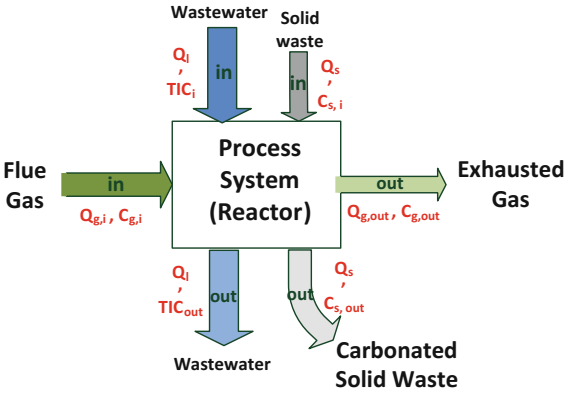

Fig. 8.2 Schematic of mass balance among gas, liquid, and solid phases (Q_g: Gas flow rate (L/min); C_g: CO_2 Concentration (%); C_{TIC}: TIC concentration in liquid phase (g/L); Q_l: Liquid flow rate (L/min); $C_{s,act}$: CO_2 capture on solid (g); L/S: Liquid-to-solid ratio (mL/g))

to be 24.5 L mol^{-1} at standard temperature and pressure (STP). The STP is defined as the temperature of 0 °C (or 32 °F) and the pressure of 760 mmHg (or 14.7 psi).

In the gas phase, CO_2 concentrations in the inlet and exhausted gas streams could be measured using a non-dispersive infrared (NDIR) CO_2 analyzer. The CO_2 removal efficiency (η, %) of the carbonation process can be calculated by Eq. (8.2):

$$\eta = \frac{\left(\rho_{CO_2,i} Q_{g,i} C_{g,i} - \rho_{CO_2,o} Q_{g,o} C_{g,o}\right)}{\rho_{CO_2,i} Q_{g,i} C_{g,i}} \times \% \tag{8.2}$$

where $\rho_{CO_{2,i}}$ and $\rho_{CO_{2,0}}$ (g/L) are the CO_2 mass density at the temperature of the inflow and exhaust gas streams, respectively; $Q_{g,i}$ (m^3/min) and $Q_{g,o}$ (m^3/min) are the volumetric flow rate of the inlet gas and exhaust gas, respectively; and $C_{g,i}$ (%) and $C_{g,o}$ (%) are the CO_2 concentration in the inlet gas and exhaust gas, respectively, which can be measured by a portable gas analyzer. If pure CO_2 gas is utilized for carbonation, since the CO_2 concentration in the input and output streams should be 99.9%, the amounts of CO_2 captured by the slurry reactor can be determined by the difference in the volumes of the gas flows measured at the inlet and outlet of the slurry reactor.

In the solid phase, the carbonation conversion (also referred to as carbonation degree) of alkaline solid wastes was determined by thermal analysis (see details in Chap. 6). Generally, the weight loss between 500 and 850 °C is caused mainly by the decomposition of $CaCO_3$ based on Eq. (8.3):

$$CaCO_{3(s)} \overset{500\sim850\,^{\circ}C}{\longrightarrow} CaO_{(s)} + CO_{2(g)} \tag{8.3}$$

For direct carbonation, it is observed that most of the gaseous CO_2 was fixed as $CaCO_3$ precipitate (i.e., solid phase). Less than 0.1% of the gaseous CO_2 was

dissolved as HCO_3^- ions and existed in the liquid phase after 120-min reaction time.

On the other hand, the mass balance of calcium species between the liquid and solid phases for indirect carbonation was determined by Eq. (8.4):

$$C_{Ca,i}V_l = C_{Ca,o}V_l + \frac{m_{CaCO_3}}{MW_{CaCO_3}} \times MW_{Ca} \tag{8.4}$$

where $C_{Ca,i}$ and $C_{Ca,o}$ are the concentrations of calcium ions in the solution before and after carbonation, respectively.

In addition, the errors of the mass balance for Eqs. (8.3) and (8.4) were evaluated by the recovery ratio (R), which is defined by Eq. (8.5):

$$R(\%) = \frac{\text{Production}}{\text{Input} - \text{Output}} \times \% \tag{8.5}$$

8.1.3 Novel Concept and Process Intensification

Mineralization of CO_2 by accelerated carbonation of alkaline wastes has the potential not only to sequester CO_2 but also to upgrade the physicochemical properties of waste streams. One of the challenges of accelerated carbonation using alkaline waste is to accelerate the reaction and exploit the heat of reaction to minimize energy and material losses. Also, pretreatments and addition of chemicals tend to consume additional energy and materials. More challenges of accelerated carbonation can be referred to Chap. 5.

To overcome the aforementioned challenges, various novel concepts and process intensification should be considered. For example, the rate of carbonation reaction can be enhanced by

- Adding acids or caustic alkali metal hydroxide
- Utilizing a bicarbonate/salt ($NaHCO_3$/NaCl) mixture
- Employing various pretreatment techniques (i.e., including physical and chemical pretreatment, electrolysis and heat pretreatment, mechanical activation methods)
- Using wastewater/brine as liquid agents
- Process intensification concepts such as
  - Thermal heat activation [7, 8]
  - Chemical activation using solvents, acids, and bases [8, 9]
  - Co-utilization with wastewater (or brine solution) [10–12]
  - Biological enhancement using enzymes and microorganisms
  - Centrifugal force [13, 14]
  - Ultrasonic vibration [9, 15, 16]
  - Electrolysis treatment [7]

In the following section, indirect carbonation and direct carbonation using alkaline solid wastes, as well as carbonation curing processes, are discussed.

8.2 Indirect Carbonation

Several effective extractants, such as acetic acid and ammonium salts (e.g., CH_3COONH_4, NH_4NO_3, NH_4SO_4, and NH_4HSO_4), are commonly used in the extraction stage [17–20]. Table 8.1 presents the types of acid and ammonium salt extractants for metal ion extraction. For ammonium salts, the acid type of the solvent is a more important factor affecting the efficiency of calcium extraction rather than the acidity of the solvent [18].

8.2.1 Acidic Extraction Process

Research on the performance of enhancing dissolution using acetic acid solutions and other chemicals has also been investigated in the literature [22, 23]. In the presence of acetic acid, the solubility of metal ions in slag was found to decrease with an increase in temperature [24]. Better chemical extractions of calcium occur at low temperatures (30 °C) at long durations (≥ 2 h). In addition, the concentration of acetic acid within the range of 0–10 wt% in the solution exhibited a dramatic

Table 8.1 Types of acid and ammonium salt extractants for metal ion extraction

Types	Extractants	Name	PH	Acidity (pK_a)	Tested concentration
Acid	HCl	Hydrogen chloride	3.72	−3.0	–
	H_2SO_4	Sulphuric acid	–	−3; 1.99	–
	HNO_3	Nitric acid	–	−1.44	–
	H_3PO_4	Phosphoric acid	–	2.148; 7.198; 12.319	–
	$ClCH_2COOH$	Haloacetic acid	–	2.86	–
	CH_3COOH	Acetic acid	5.32	4.76	–
Base (salt)	NH_4NO_3	Ammonium nitrate	9.8–10.5	Solid form	0.5–1 M [18]
	CH_3COONH_4	Ammonium acetate	9.5	Solid form	0.5–1 M [18]
	NH_4Cl	Ammonium chloride	9.0–9.6	Solid form	2 M at 60 °C [21]
	$(NH_4)_2SO_4$	Ammonium sulfate	9.6	Solid form	0.5–1 M [18]

effect upon the extraction of calcium [24]. Compared to only 30 mg/L of calcium after 2 h without acetic acid addition, 4000 mg/L of calcium can be extracted in 5 min using an aqueous solution of 10 wt% acetic acid. However, a further increase of acetic acid concentration to 33.3 wt% did not result in a significant difference from that of 10 wt% acetic acid. Therefore, approximately 6–7 mL glacial acetic acid per gram of slag is suggested for effective calcium extraction [24]. After extraction, a maximum carbonation conversion of 86% can be achieved under a CO_2 concentration of 10% at 30 °C, with a $CaCO_3$ purity of 99.8%. Roughly 4.7 tons of steel slag are consumed for one ton CO_2 capture, with 2.3 tons of end $CaCO_3$ products and 3.4 tons of residual slag [23].

8.2.2 Base Extraction Process

In base extraction process, ammonium chloride (NH_4Cl) is commonly used due to its relative ease of recycling. The ammonia being stripped out during extraction step can be recycled and utilized for pH adjustment in order for the leachate to minimize the consumption of ammonia during the operation [21]. When ammonium chloride is used, the extraction can be improved as the particle size of slag decreased and the reaction temperature increased, with a maximum extraction yield of 60% [25]. As the extraction reaction proceeded, the deposition of an inert layer (such as SiO_2) formed on the reactive surface, thereby limiting further diffusion of extractant into slag particles [26].

The overall carbonation reactions of leachate can be expressed as shown in Eq. (8.6):

$$2\,NH_4OH + (Ca, Mg)Cl_2 + CO_2 \rightarrow (Ca, Mg)CO_3 + 2\,NH_4Cl + H_2O \tag{8.6}$$

In fact, at the beginning, the CO_2 will react with NH_4OH, as described in Eqs. (8.7) and (8.8):

$$NH_4OH_{(aq)} + CO_{2\,(aq)} \rightarrow NH_4HCO_{3\,(aq)} \tag{8.7}$$

$$2\,NH^+_{4\,(aq)} + HCO^-_{3\,(aq)} + OH^-_{(aq)} \rightarrow (NH_4)_2CO_{3(aq)} + H_2O_{(aq)} \tag{8.8}$$

As carbonation proceeds, the dissolved CO_2 will continuously consume OH^- in solution, thereby inhabiting reaction (8.8). In this case, the produced NH_4HCO_3 (Eq. 8.7) will begin to react with calcium/magnesium ions to form calcium/magnesium bicarbonate, which is described in Eq. (8.9)

$$(Ca, Mg)^{2+}_{(aq)} + 2\,HCO^-_{3(aq)} \rightarrow (Ca, Mg)(HCO_3)_{2(aq)} \tag{8.9}$$

The efficiency of calcium extraction was found to be higher in the order of $(NH_4)_2SO_4 < NH_4Cl < CH_3COONH_4 < NH_4NO_3$, regardless of their solution

concentrations [18]. Similarly, the efficiency of various extractants on the carbonation behavior was found to be in the same sequence [18]. It was noted that the maximum CO_2 capture capacity can reach around 210 kg CO_2 per ton of slag, with the consideration of the contribution of $Mg(HCO_3)_2$ in capturing CO_2 [21]. In this case, the precipitates obtained under optimized carbonation conditions were rich in $CaCO_3$ with a purity of 96 ± 2%.

On the basis of experimental analysis, the energy consumption of the proposed process using ammonium chloride was estimated as 300 kWh/ton-CO_2 [25]. This value is smaller than other CO_2 sequestration processes; for instance, 470–640 kWh/t-CO_2 for amine absorption and geological sequestration [27].

8.2.3 Multistage Indirect Carbonation

Multistage indirect carbonation, in the presence of additives, can reach high carbonation efficiency under mild operating conditions within a short residence time [28, 29]. It was noted that high-purity carbonate precipitates (e.g., spherical vaterite) can be generated by multistage indirect carbonation [18]. For example, two-stage (or so-called pH swing) indirect carbonation processes are one type of the multistage indirect carbonation. They have been evaluated to optimize the efficiency of the dissolution and carbonation processes, as well as to achieve a pure precipitate product for specific industrial applications. The pH-swing using a weak base—strong acid solution, with a fine particle size (e.g., less than 63 μm) at 80 °C, in which the maximum calcium extraction ratio and carbonation conversion achieved, was 60 and 70%, respectively [25].

The requirement of an energy-intensive process for chemical regeneration might be a limiting factor for large-scale deployment. It was noted that energy and chemical costs could be reduced by carrying out the reaction between hydroxide and CO_2 at high pressure (i.e., 2.5 MPa) and temperature (i.e., 450 °C) [30]. This potentially makes the hydroxide route technically achievable on an industrial scale.

8.3 Direct Carbonation

Recently, the ex situ direct aqueous carbonation has aggressively developed for carbon fixation and utilization. There is more than enough natural ore on Earth to sequester the CO_2 emissions from all fossil fuels [6]. However, the existing methods for mineral carbonation are still expensive due to the energy-intensive mining process. To effectively lower the carbonation process, alkaline solid wastes are thus used in the carbonation process because they are relatively cheaper

feedstocks than natural ores. Accelerated carbonation involves the following three steps (see details in Chap. 5).

- Calcium leaching from alkaline solid matrix into solution
- Gaseous CO_2 dissolution in solution
- Calcium carbonate precipitation

For various types of processes, the mass transfer steps, i.e., CO_2 dissolution into solution and the diffusion of reactants in solid matrix, are typically considered to be the rate-limiting step. Consequently, it is essential to improve the mass transfer phenomena to achieve a rapid reaction.

Accelerated carbonation has been focused on assessing and maximizing the performance of CO_2 capture capacity by optimizing the operating conditions, such as pressure, temperature, liquid-to-solid (L/S) ratio, gas humidity, gas flow rate, liquid flow rate, particle size, and solid pretreatment in the literature [1, 28, 31–34]. In the following part, several important processes, such as slurry reactor, autoclave reactor, high-gravity carbonation, and ultrasonic technology, are introduced.

8.3.1 Autoclave Reactor

A schematic diagram demonstrating the carbonation of alkaline solid wastes in an autoclave reactor is shown in Fig. 8.3. CO_2 was injected continuously into the reactor at a designated pressure and a constant flow rate. The key operational factors, including the reaction time (t), liquid-to-solid ratio (L/S), reaction temperature (T), CO_2 pressure (P), and initial pH, are varied systematically with the various feedstocks to minimize energy and chemical consumption.

In the case of operation at 160 °C and 700 psig, the carbonation of the ultra-fine slag (UFS), fly ash slag (FAS), and blended hydraulic cement slag (BHCS) are 38.1, 34.7, and 68.3%, respectively [35]. Accordingly, the actual CO_2 capture capacities per kg of dry solid are approximately 130, 110, and 280 kg CO_2 for the UFS, FAS, and BHCS, respectively. The carbonation reaction exhibited a stationary phase after 60 min because of the formation of a calcium-depleted SiO_2 rim on the surface of particle. This would strongly block the reactive surface sites, thereby inhibiting the further release of calcium ions from the particle.

The CO_2 pressure in the autoclave reactor could vary between two various conditions: a normal condition (700 psig) and a supercritical condition (1300 psig). The conversion of alkaline solid wastes in supercritical CO_2 was found to be slightly less than that in normal CO_2 [35], due to the inhibition of $CaCO_3$ crystal growth under this supercritical pressure. However, in general, a high pressure increases the rate of the carbonation reaction, which precludes the formation of $CaCO_3$ crystals and inhibits the reaction. In the supercritical conditions (e.g.,

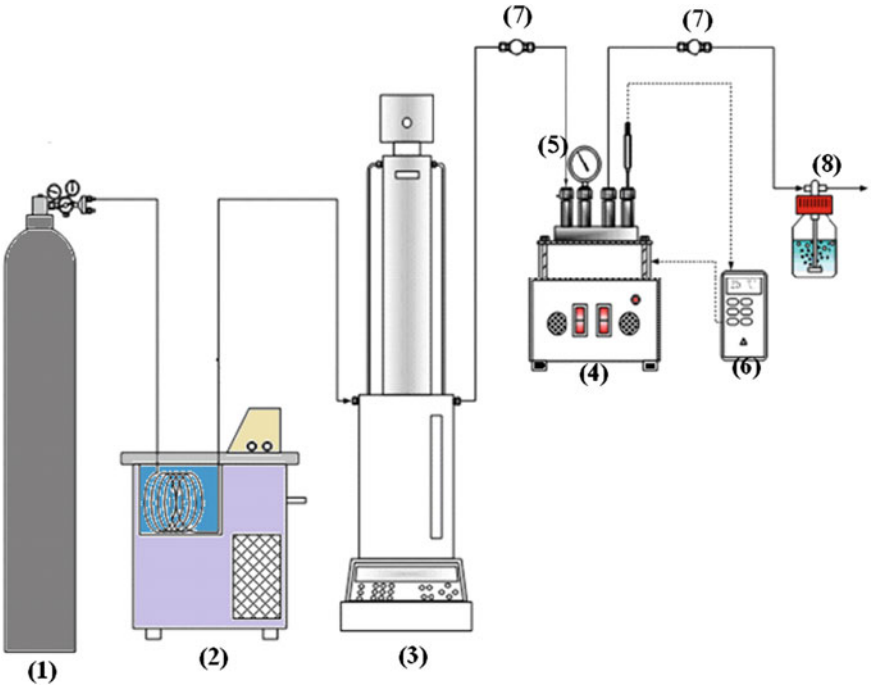

Fig. 8.3 Schematic diagram of the experimental setup of autoclave reactor for the carbonation of alkaline solid wastes (*1*) gas cylinder; (*2*) circulating bath; (*3*) syringe pump; (*4*) magnetic stirrer and heater; (*5*) autoclave reactor; (*6*) thermo couple and pH analyzer; (*7*) needle valve; and (*8*) vent to hood

1300 psig), the CO_2 fluid has a relatively higher solubility of liquid and lower dynamic viscosity of gas. The conversion of BHCS increases due to its superior CO_2 solubility at higher pressure and temperatures. The temperature significantly influenced the carbonation conversion of BHCS, with increasing temperatures resulting in higher conversions.

8.3.2 Slurry Reactor

A slurry reactor contains fine solid particles suspended in a liquid. It is frequently used in the chemical and/or biochemical industries due to its ability to enhance mass transfer [36]. The first application of the two-phase fluidization system was made by Winkler in 1922. The gas–liquid–particle three-phase system was then developed, which seems to be a more efficient tool for a chemical reactor [37]. Compared to that using an autoclave reactor, slurry reactor can provide a higher

contact frequency between CO_2 and the feedstock, and can be operated in a continuous mode at relatively low (ambient) temperature and pressure.

8.3.2.1 Performance Evaluation

Figure 8.4 shows the schematic diagram of the slurry reactor for accelerated carbonation of alkaline solid wastes. Normally, CO_2 is injected into the slurry reactor continuously at 101.3 kPa (ambient) and a constant flow rate. The key operation factors generally include the reaction time (or hydraulic retention time), liquid-to-solid (L/S) ratio, slurry volume, reaction temperature, and gas flow rate.

In the slurry reactor system, a carbonation conversion of 53.8% for steel slag can be achieved at an L/S ratio of 20:1 (with DI water) and a CO_2 pressure of 0.1 MPa at 25 °C for 60 min [38]. The carbonation uptake at atmospheric pressure exceeded 80% of the reference 56-day value after 7 days of exposure and had reached 95% within 28 days. Although the atmospheric pressure carbonation treatment provided a slightly lower carbonation conversion, it was accomplished with a gas of low pressure and dilute CO_2 concentration [39]. In addition, with the consideration given to the grinding process and blowers, the energy consumption for capturing 1 ton of CO_2 using the slurry reactor is estimated to be 180.3 kWh (in the case of MSWI bottom ash) [40]. It thus suggests that an economical approach to sequestering CO_2 in alkaline solid wastes with minimum energy consumption and direct use of flue gas could be achieved.

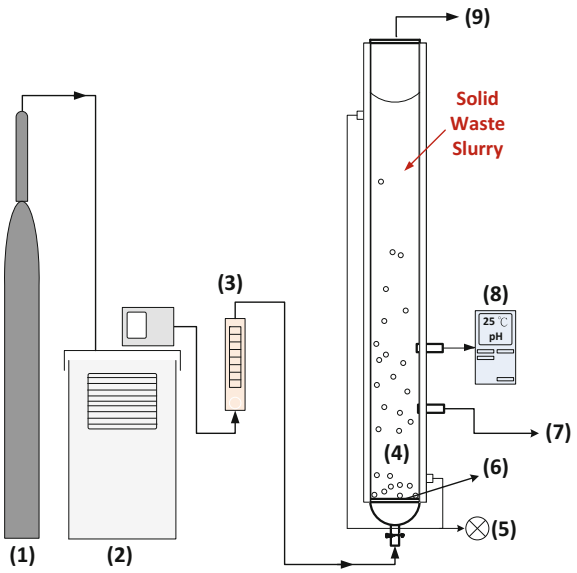

Fig. 8.4 Schematic diagram of the experimental setup of slurry reactor for accelerated carbonation of alkaline solid wastes (*1*) gas cylinder; (*2*) circulating bath; (*3*) rotameter; (*4*) slurry reactor; (*5*) heating jacket; (*6*) gas distributor; (*7*) sampling; (*8*) thermo couple and pH analyzer; and (*9*) vent to hood

8.3.2.2 Key Operating Factors

Since the mass transfer between the liquid and gas phases could be enhanced by increasing the CO_2 flow rate, the conversion of steel slag was observed to improve when the flow rate increased [11]. However, the conversion decreases moderately with further increasing flow rate in the slurry reactor [38]. This is because the channeling effect in the slurry reactor becomes significant at a high flow rate, resulting in a poor gas–liquid mass transfer rate and a decrease of carbonation conversion. Moreover, a higher CO_2 flow rate delivered a greater amount of CO_2 into the reactor. At a constant reaction time, the pH value drops more rapidly with a high flow rate than with a low flow rate, which is unfavorable to carbonation reaction. Therefore, the flow rate should be limited to a certain value that is able to make the slurry reactor in a fluidization mode.

The carbonation conversion of alkaline solid waste largely depends on the reaction temperature since the temperature would affect several system parameters, including the reaction kinetics, equilibrium, CO_2 dissolution, and calcium leaching simultaneously. In general, reaction rate would significantly increase with increasing reaction temperature, since the reaction rate constant exponentially increases with increasing temperature as expressed by the Arrhenius equation. However, because the carbonation is an exothermic reaction, an increase in temperature may also lead to a decrease in the equilibrium constant based on Le Chatelier's principle. Similarly, the rate of the CO_2 dissolution and the calcium ion leaching at higher temperature would decrease and increase, respectively.

It suggests that the maximum carbonation conversion of steel slag should be at a temperature of 60 °C [38]. In this case, the carbonation reaction can be generally categorized into two main regimes:

- Temperatures below 60 °C: The carbonation conversion increased with increasing reaction temperature due to the higher leaching rate of calcium ions. The $CaCO_3$ crystallization reaction was thus accelerated at higher temperature in this regime (30–60 °C).
- Temperatures above 60 °C: Boiling in the slurry reactor was accompanied by the low dissolution of CO_2, resulting in a decrease in the carbonation conversion. In this regime (60–80 °C), the CO_2 solubility is likely to be the key factor affecting the carbonation conversion.

The liquid-to-solid (L/S) ratio represents the weight ratio of water solution to alkaline solid wastes. It suggests that the L/S ratio should be greater than 5 mL/g to achieve a better carbonation of alkaline solid wastes [40]. Otherwise, the significant amounts of foreign ions would dissolve in the slurry, resulting in a competitive reaction and lowering the rate of calcium dissolution. It was noted that a maximum carbonation conversion of steel slag achieved in the slurry reactor was 89% at an L/S ratio of 20. When the L/S ratio was lower than 20, the slurry could not mix well in the slurry reactor, leading to poor mass transfer between liquid and solid phases. However, when the L/S ratio was higher than 20, a lower leaching concentration of

calcium ions in solution occurred since the amount of solid waste per unit volume of liquid solution was lower.

8.3.3 *High-Gravity Carbonation (HiGCarb)*

A rotating packed-bed (RPB) reactor is designed to enhance mass transfer between gas and liquid phases via high centrifugal acceleration. RPB reactor can provide a mean acceleration of up to 1000 times greater than the force of gravity, thereby leading to the formation of thin liquid films and tiny liquid droplets (microscale to nanoscale) [41–47]. With this feature, the mass transfer between gas (CO_2) and aqueous solution in an RPB reactor can be significantly improved, resulting in a high capture efficiency within a short contact period. Moreover, using an RPB reactor can intensify the mixing of microscopic amounts of material by molecular diffusion (so-called micromixing efficiency) due to the formation of thin film flow on the packings. As a result, the excellent micromixing abilities of the RPB reactor can be applied for numerous applications of contact between two different phases (also refer to Chap. 17 for details), such as

- Absorption: for example, CO_2 capture through the use of absorbents (e.g., alkanolamine, piperazine, and NaOH).
- Distillation: for example, petrochemical process.
- Stripping: for example, ammonia stripping.
- Ozonation: for example, water disinfection.
- Biodiesel production: for example, transesterification.

In the case of accelerated carbonation using an RPB reactor, it involves in a three-phase mixing (i.e., gas, liquid, and solid phases) system. Since the aqueous carbonation of alkaline solid wastes was believed to be a diffusion-controlled reaction, an RPB reactor was introduced to improve the mass transfer rate among phases due to its high centrifugal forces and effective micromixing ability. This approach using an RPB reactor for accelerated carbonation of solid wastes is so-called high-gravity carbonation (HiGCarb) process [10, 13, 14, 48, 49], as shown in Fig. 8.5. The reactants are presumed to be intensively mixed within a short time, typically $\sim$1 min, in the packed-bed rotator while the carbonation reaction proceeds quickly.

8.3.3.1 Batch Operation

Figure 8.6 shows the schematic diagram of experimental setup for HiGCarb process. The slurry of alkaline solid waste is constantly stirred in all experiments. In the experiments, CO_2 gas stream flows inward from the outer edge of the RPB under a pressure driving force, while the slurry of alkaline solid waste is pumped

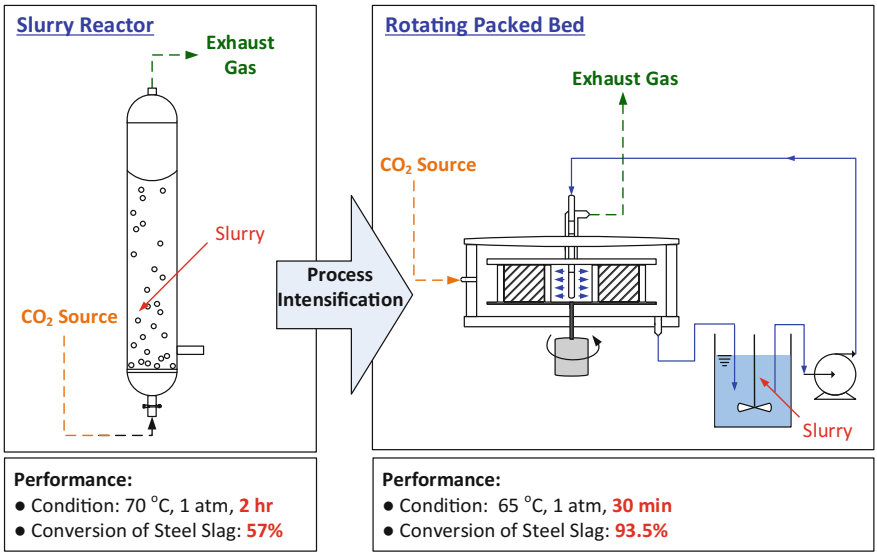

Fig. 8.5 Schematic diagram of process intensification via rotating packed-bed reactor for accelerated carbonation, i.e., high-gravity carbonation (HiGCarb) process

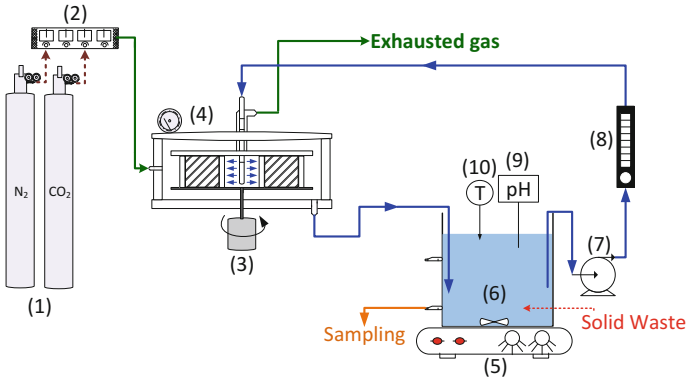

Fig. 8.6 Schematic diagram of the experimental setup for high-gravity carbonation (HiGCarb) process (*1*) gas cylinder; (*2*) mass controller; (*3*) rotor; (*4*) high-gravity RPB reactor; (*5*) stirring and heating machine; (*6*) slurry storage tank; (*7*) pump; (*8*) rotameter; (*9*) pH meter; and (*10*) thermometer

from the repository to the inner edge of the RPB. The slurry moves outward and leaves from the outer edge of the RPB under centrifugal force. As shown in Fig. 8.5, both CO_2 and slurry are mixed countercurrently within the RPB, in which CO_2 is dissolved in the liquid phase and reacts with the reactive species dissociated

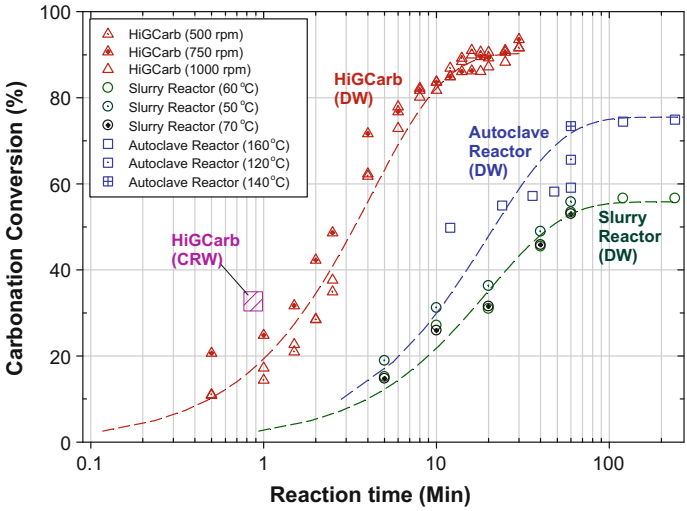

Fig. 8.7 Effect of reaction time on carbonation conversion of steel slag using autoclave reactor [35], slurry reactor [38], and high-gravity carbonation (HiGCarb) with cold-rolling wastewater [13] and DI water [49]

from the slag. The slurry is discharged from the bottom of the RPB, whereas the exhausted CO_2 streams are expelled from the top.

Chang et al. [49] conducted a batch-modulus HiGCarb process under low temperature (i.e., less than 70 °C) at ambient pressure. A maximum basic oxygen furnace slag (BOFS) carbonation conversion of 94% can be achieved by the HiGCarb process at 65 °C for 30 min, corresponding to a capture capacity of 290 kg CO_2/t-BOFS. The experimental results revealed a rapid reaction rate during the first 5 min at a gas-to-slurry ratio of 20 and an approximately constant rate thereafter. In general, an increase in the rotation speed would not only enhance the mass transfer of CO_2 from the gas phase to the liquid phase, but would also reduce the residence time distribution (RTD) of the slurry within the packed bed. Therefore, an optimal rotation speed should be determined to balance the mass transfer and reaction kinetics.

Figure 8.7 shows the comparison of carbonation conversion for steel slag using autoclave reactor, slurry reactor, and HiGCarb process with cold-rolling wastewater (CRW) and DI water. The HiGCarb process evidenced a relatively higher CO_2 removal efficiency and carbonation conversion of alkaline solid waste with a short reaction time than those in an autoclave or a slurry reactor [13, 34, 48, 49]. It was also found that carbonation conversion of steel slags could be significantly enhanced by using wastewater (i.e., CRW) in the HiGCarb process [13].

8.3.3.2 Continuous Field Operation

For continuous operation using the HiGCarb process, CO_2 fixation and waste treatment at a blast furnace plant in steel industry are performed using the BOFS. In this operation tests, the packed bed is in horizontal rotation with a mean diameter and height of 46.5 and 19.9 cm, respectively. The maximal rotation speed of the packed bed is designed as 900 rpm, to provide a centrifugal acceleration of up to 2065 m/s^2 (about 210 g). The CO_2 source with an average concentration of 30 ± 2% was supplied directly from a hot-stove furnace at the steel industry; no capture or concentrated processes were required in advance.

High CO_2 removal efficiency can be achieved with a retention time of less than 1 min under ambient temperature and pressure conditions [13]. A maximal CO_2 removal of 97% was achieved at a G/L ratio of 40, with a capture capacity of 165 kg CO_2 per day, as shown in Fig. 8.8. The CO_2 removal efficiency moderately increases as the rotation speed increases up to 500 rpm. This is due to the reduction of mass transfer resistance (i.e., reduced liquid film thickness) by increasing the rotation speed within this range, which is favorable to the carbonation reaction [13].

In addition, the increase of slurry flow rate can also improve the liquid-side mass transfer. In the HiGCarb process, a higher slurry flow rate brings a faster initial radial velocity of slurry droplets and causes a relatively thinner liquid film and a higher relative velocity between the slurry and the CO_2, thereby enhancing the mass transfer between the liquid and gas and intensifying the micromixing. However, it

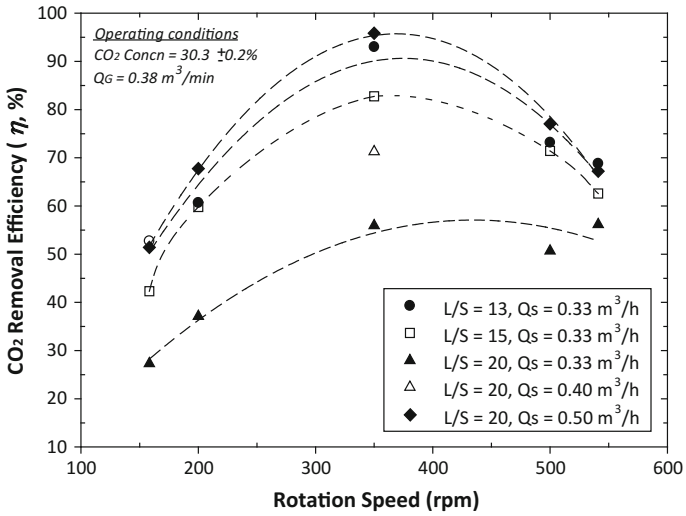

Fig. 8.8 Influence of rotation speed, liquid-to-solid (L/S) ratio, and slurry flow rate on CO_2 removal efficiency in hot-stove gas using high-gravity carbonation process. Reprinted with the permission from ref. [50]. Copyright 2015 American Chemical Society

also results in a lower RTD within the packing zone of the RPB reactor at higher slurry flow rates. This implies that the overall mass transfer resistance of carbonation reaction in the HiGCarb process might be mainly led on the liquid-phase side according to the two-film theory. Furthermore, the amount of calcium left in solid waste decreased as the calcium rapidly dissolved into solution, thereby resulting in a diminished concentration gradient needed to maintain the dissolution rate.

Similar observations can be found by adjusting other operating parameters. At higher gas flow rates, an increase in gas–liquid contact area and a reduction in gas-phase mass transfer resistance occur. However, the CO_2 removal efficiency was observed to decrease at a higher gas flow rate (i.e., a higher G/L ratio). It is confirmed that the high-gravity process is a liquid-side mass transfer controlled reaction. This suggests that both the rotation speed and G/L ratio should be the key factors for scale-up design of the HiGCarb process.

8.3.4 Ultrasonic Carbonation

Since the carbonation reaction is regarded as diffusion controlled (i.e., mass transfer limited), intensification of mass transfer efficiency among phases was essential to improve CO_2 capture capacity and reduce energy consumption and operating costs. A slurry reactor incorporated with ultrasound vibration has been introduced to accelerate the precipitation rate of calcium carbonate via ultrasonic irradiation [9, 15, 16, 51]. The results indicate that the efficiency of physical mixing, particle breakdown, and removal of passivation layers increased with sound waves with frequencies in the range of 16–100 kHz. Therefore, a better conversion can be achieved in a shorter time compared to that without ultrasound; for instance, the carbonation conversion of combustion ashes increased from 27 to 83% with ultrasound for 40 min [51].

8.3.5 Biologically Enhanced Carbonation

8.3.5.1 Microorganism

Microorganisms are the microscopic living organism, such as bacteria, protozoa, and algae. The anaerobic and aerobic bacteria can positively promote carbonation by enhancing the solubility and dissolution of minerals [52]. The absorption of cations by a cell wall (net negative) can increase the cation concentration within the cell, which can be used to facilitate mineral precipitation. The “carbonation ponds” or “basins” with a high alkalinity are designed to use a natural cyanobacteria-dominated consortium for the photoautotrophs to thrive and precipitate carbonates [53]. This process also can serve as silicon sinks by the formation of mineralized cell walls (i.e., frustule) from $[SiO_2{\cdot}nH_2O]$ in the bioreactor.

Another approach is to utilize algae and cyanobacteria to perform photosynthesis in the presence of sunlight. The sunlight is used as energy by proteins (so-called reaction centers) to convert gaseous CO_2 into biosubstance (i.e., chemical energy) [52, 53]. The reaction centers (proteins) contain green chlorophyll pigments, which can strip electrons from suitable substances such as water to produce water. This part of mechanism is called light reactions. Then, the CO_2 can be used to convert into carbohydrate molecules, such as sugar, where the chemical energy is stored in. This part of mechanism is called light-independent (dark) reactions, or Calvin–Benson cycle, as shown in Eq. (8.10).

$$3\,CO_2 + 9\,ATP + 6\,NADPH + 6\,H^+ \rightarrow C_3H_6O_3 - \text{phosphate} + 9\,ADP + 8\,P_i + 6\,NADP^+ + 3\,H_2O \tag{8.10}$$

Usually, plants can convert light energy into chemical energy with a photosynthetic efficiency of 3–6% [54]. For comparison, solar panels can convert light energy into electric energy at an efficiency of 6–20% for large-scale production and >40% in the laboratory scale.

8.3.5.2 Enzymatic Carbonation

Typically, the supply of CO_2 is limiting the rate of carbonation due to the slow kinetics of CO_2 dissolution. Enzymatic carbonation relying on carbonic anhydrase (CA) could be an effective approach to overcoming the above process hurdle, even in an industrial environment, or when utilized in an open-air environment. The CA family can catalyze the rapid interconversion of gaseous CO_2 and water to form bicarbonate (HCO_3^-) and protons (H^+), as shown in Eq. (8.11). There are at least five distinct CA families (i.e., α-CA, β-CA, γ-CA, δ-CA, and ε-CA), where these families exhibit no significant amino acid sequence similarity. The catalytic rates of various CA enzyme families typically range between 10^4 and 10^6 reactions per second [55].

$$CO_{2(g)} + H_2O_{(aq)} \xrightarrow{\text{Carbonic Anhydrase}} H_2CO_{3(aq)} \rightarrow HCO^-_{3(aq)} + H^+_{(aq)} \tag{8.11}$$

It is noted that the CA enzyme could enhance the carbonation of Ca- and Mg-bearing materials [56, 57]. For example, a CA enzyme-based membrane system was able to remove 90% of the CO_2 supplied [58]. However, the instability and high material costs of CA are still the challenges for practical and large-scale applications [28].

8.4 Integrated Carbonation with Brine (Wastewater) Treatment

Brine or wastewater is a saline-based waste solution (e.g., total dissolved solid is generally more than 50,000 mg/L) produced from industrial procedures, such as oil and natural gas extraction (known as oil-field brines). It can be used as the liquid agents in the carbonation reaction [12, 59–61]. Most wastewater treatments use chemicals as a neutralizing agent to adjust pH of wastewater and enhance metal precipitation. However, the use of chemicals carries with it a high economic and environmental cost because it is a "resource" and not a "residue."

The wastewater or brine solution can be used for accelerated carbonation process to enhance (1) the rate of calcium ion leaching from solid wastes, or (2) gaseous CO_2 dissolution into the liquid phase. The total dissolved solid (TDS) in wastewater is generally higher than that in tap water due to high concentrations of anions and cations. The criteria of wastewater and/or brine property for carbonation are illustrated as follows [12, 61]:

- A pH of the solution over 9.0 is favored to the precipitation of carbonate because CO_3^{2-} dominates under a basic condition.
- The selected solution should contain neither bicarbonate nor carbonate ions.

Under the appropriate conditions, CO_2 would dissolve in the brine solution to initiate a series of reactions that ultimately lead to the bonding of carbonate ions to various metal cations inherent in brine or wastewater to form carbonate precipitates, such as calcite ($CaCO_3$), magnesite ($MgCO_3$), and dolomite ($CaMg(CO_3)_2$).

8.4.1 Enhanced Calcium Leaching for Carbonation

The carbonation reaction can be enhanced by coupling with brine solution and/or wastewater, such as metalworking wastewater. Pan et al. [48] found that the leaching concentration of calcium ions in metalworking wastewater was higher than that in DI water, thereby resulting in a greater carbonation reaction rate and higher CO_2 capture capacity. Figure 8.9 shows the leaching concentration of calcium ions in DI water and metalworking wastewater (e.g., CRW) for different particle sizes of steel slag (i.e., BOFS). The leaching rate and capacity of calcium ions from steel slag in metalworking wastewater were greater than that in tap water. The measured pH values of metalworking wastewater ranged from 11.20 to 11.87. A maximum Ca^{2+} concentration of 2600 mg/L was measured in the alkaline wastewater with a particle size of steel slag less than 125 μm. The leaching of metal ions from the solid waste into solution would be higher with smaller particle size.

The high concentration of Na^+ and Cl^- in wastewater might accelerate the leaching behavior of Ca-bearing phases in solid wastes. The presence of inorganic ionic species in solution, such as sodium and chloride, can promote the dissolution

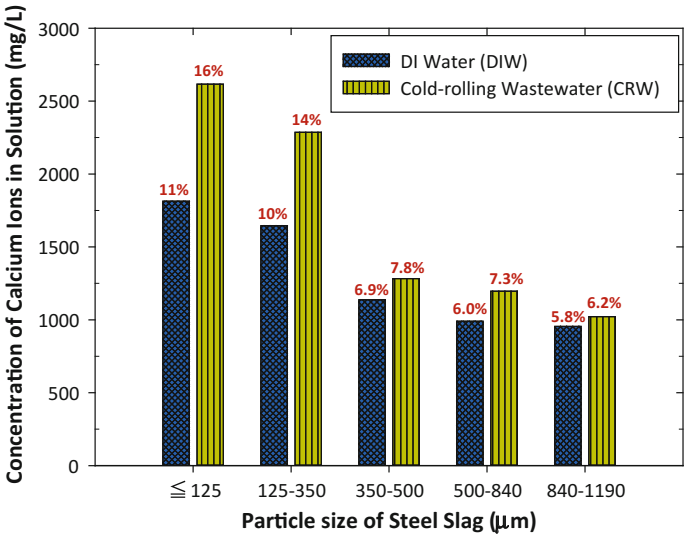

Fig. 8.9 Leaching concentrations of calcium ion in deionized (DI) water and cold-rolling wastewater under different particle sizes of steel slag for 90 min. Percentages shown on each bar represent the fraction of leaching concentration in totally leaching concentration

of silicate-bearing minerals due to the formation of surface complexes, leading to the reductive (and oxidative) dissolution of minerals [62–64]. O'Connor et al. [65] found that the addition of the sodium chloride can improve the extent of the carbonation reaction. Similarly, the use of the caustic alkali metal hydroxide can enhance the carbonation of metal silicates via the following mechanism [66]:

$$3CaSiO_{3(s)} + \underline{\mathbf{Na}}OH_{(aq)} + CO_{2(g)} \rightarrow CaCO_{3(s)} + \underline{\mathbf{Na}}Ca_2Si_3O_8(OH)_{(s)} \quad (8.12)$$

Jo et al. [67] found that Ca leaching from ordinary Portland cement (OPC) in aqueous solution and the hydration of C–S–H into $Ca(OH)_2$ in the OPC were enhanced by the presence of NaCl. In the presence of 0.2–2.0 M NaCl, the carbonation of OPC can thus be enhanced by 7.5–18.4%, in terms of the amount of $CaCO_3$ precipitation, which might be attributed to the increase in C–S–H dissolution by interaction with chloride ions. This suggests that a greater reactivity of the calcium-bearing complex toward chloride than other ions was found, thereby resulting in greater dissolution rates of minerals in the presence of chloride. Likewise, Nyambura et al. [68] suggest that the carbonation conversion of solid wastes is higher in the brine/solid residues system, compared to the water/solid residues.

8.4.2 Enhanced Carbonation Conversion of Alkaline Solid Wastes

In general, the carbonation conversion in the brine/solid residues system is higher than that in the water/solid residues [11, 50, 68]. O'Connor et al. [65] found that the addition of sodium chloride can enhance the carbonation reaction. Similarly, the concentrations of sodium and chloride in alkaline wastewater are generally higher than those in DI water. As a result, Nyambura et al. [68] found that the carbonation conversion in the brine/solid residues system should be higher than that in the water/solid residues. The carbonation efficiency in the fly ash (FA)/brine system under a pressure of 4 MPa at 30 °C was 86%, which was superior to the water/brine system (i.e., 68.2%) [68].

A maximum capture capacity of 283 g CO_2 per kg slag, corresponding to a carbonation conversion of 89%, can be achieved in alkaline wastewater with a reaction time of 120 min at 25 °C and an L/S ratio of 20 [11]. The highest carbonation conversion was observed in the alkaline wastewater system, compared to the neutralized effluent water and DI water. This might be attributed to more CO_2 dissolved in the liquid phase under higher pH, thereby enhancing the carbonation reaction. It thus suggests that the carbonation reaction of steel slag was enhanced more in the alkaline wastewater system than in the DI water system.

8.4.3 Improved Water Quality After Carbonation

Although the concentration of Fe, Sr, and Ba decreases in the solution, iron hydroxide, strontium carbonates, and barium carbonates were not detected by XRD, most likely, due to the small amounts of iron (i.e., 434 ppm) and barium (i.e., 917 ppm) present in the fresh brines [61]. After carbonation, the concentrations of TIC and magnesium in wastewater increased significantly, while the concentrations of sodium and calcium were found to be decreased as well as the pH value. The decrease of the calcium concentration after carbonation might be caused by the formation of the calcium carbonate in the course of carbonation. In addition, the concentrations of potassium, iron, and nitrate remained roughly constant for wastewater. It was noted that the CO_2 was absorbed into the slurry, thus leading to the formation of calcium carbonate precipitations and the increase of the TIC concentration in the slurry [11].

8.5 Carbonation Curing Process

The use of supplementary cementitious materials (SCMs) is a sustainable practice to make environmentally friendly cement and concrete industries. Aside from using CO_2 in direct carbonation of solid wastes for the production of SCMs, the CO_2 can be used in the curing process during the preparation of cement mortar, so-called "carbonation curing" process. Carbonation is a common type of attack in mortars and concretes, where CO_2 penetrates into the mortar and reacts with Ca^{2+} from calcium hydroxide (CH), calcium silicate hydrate (C–S–H), and the hydrated calcium aluminates and ferroaluminates. As a result, various types of calcium carbonate ($CaCO_3$), silica gel, and hydrated Al/Fe oxides can be formed during carbonation curing.

The carbonation curing process can significantly improve the mechanical properties and durability of the cementitious materials. This early-age carbonation in curing is the reaction between calcium silicates or early hydration products with carbon dioxide producing a hybrid binder structure of calcium silicate hydrates and calcium carbonates [69]. With the carbonation curing process, the initial porosity of mortar reduces since the volume of the formed $CaCO_3$ is about 12% greater than the volume of the original CH phase. This would result in a higher compressive strength at early ages of carbonation, thereby preventing further CO_2 diffusion and carbonation attack [70, 71]. Ghouleh et al. [72] suggest that the improvement on the early strength could be attributed to carbonation of the γ-C_2S component in solid waste, as shown in Eq. (8.13).

$$2(2CaO \cdot SiO_2) + CO_2 + 3\,H_2O \rightarrow 3\,CaO \cdot 2SiO_2 \cdot 3H_2O + CaCO_3 \qquad (8.13)$$

However, if the porosity of the carbonated pastes is sufficiently high to permit constant CO_2 diffusion, the CH will be depleted and the interlayer calcium from C–S–H will react with CO_2. Polymerization of the silicate chains in C–S–H occurs afterward and causes a volumetric shrinkage, resulting in material cracks and coarse porosity [70].

Several studies have been carried out to evaluate the effect of carbonation curing on the properties of blended cement [73] and concrete masonry [69]. Table 8.2 presents the performance of carbonation curing for cements or concretes with various types of solid wastes. Wu et al. [74] demonstrated that, after carbonation curing, the blended cement with steel slags exhibited higher strength and eligible soundness. With carbonation curing process, early hydration products in cement are converted to a crystalline microstructure, and subsequent hydration transforms amorphous carbonates into more crystalline calcite [69].

In addition, Mo et al. [73] showed that carbonation curing using higher pressure CO_2 could result in faster strength development due to the rapid penetration of CO_2 and carbonation of blended cement. Salman et al. [78] found that a higher strength for cylindrical specimens (d = 55 mm, h = 75 mm) made out of compressed continuous casting slag could be achieved within 6 h by the carbonation curing

Table 8.2 Carbonation curing process for various types of alkaline solid wastes as construction cements in cement or concrete

Waste sources	Carbonation curing condition (pure CO_2)[a]	Feedstock and carbonation process	Substitution ratio (wt%)	Performance and product properties[c]	References
Steel slag and blast furnace slag	0.54 MPa at 88 °C for 2 h, RH 12.6%	Water content of 12–13%, with 2% additives	Steel slag: blast furnace slag = 41:57	f_c = 2.1 MPa (uncarbonated) and 18.4 MPa (carbonated) CO_2 gain = 17.7%	[74]
Steel slag	0.54 MPa at 20 °C for 2 h	Particle size = 5–24 μm; L/S ratio = 0.125; eligible autoclave soundness	n.r.[b]	f_c = 4.65 MPa (uncarbonated); 44.97 MPa (carbonated) Capacity: 107.9 CO_2 g/kg specimen Porosity: 21.8% → 13.3%	[75]
Steel slag	0.32 MPa at 86 °C for 2 h	Particle size < 75 μm; optimal water content = 19%	50	f_c = 4.0–6.3 MPa at 3-d; 18.5–24.6 MPa at 28-d CaO_f = 3.9% → 1.1%	[76]
Steel slag	0.15 MPa for 2 h	Particle size (SS) = 212 μm; w/s ratio = 0.15; compacted by 16 MPa; sealed hydration for 28 d	100	f_c = 0.7 MPa (uncarbonated curing); 109.3 MPa (carbonation curing) CO_2 uptake of SS = 13.94 wt%	[72]
Argon oxygen decarburization slag	0.8 MPa at 80 °C for 5 h	Normal curing (5% CO_2 at 1 atm, 22 °C, RH 80%) followed by carbonation; particle size < 500 μm; w/s ratio = 0.15 (wt)	n.r.[b]	f_c = 40.7 MPa CO_2 uptake of AODS = 6.72 wt%. Porosity: 35.7% (3 d) → 33.9% (3 weeks) Precipitation of calcite, aragonite and vaterite	[77]
Hydrated fly ash	0.1 MPa at 23 °C for 14 d, RH 55-65%	Normal curing (23 °C, RH 98%) followed by carbonation; water to binder = 0.4	Fly ash: MgO: cement = 1:1:3	f_c = 62.9 MPa (uncarbonated curing); 67.2 MPa (3 h carbonation curing); 90.0 MPa (14 d carbonation curing) Pore volumes reduced by 32.1% (3 h)	[73]

[a] *RH* relative humidity
[b] *n.r.* not report
[c] f_c = compressive strength of mortar; f_t = tensile strength of mortar; f_f = flexural strength of mortar

process at higher temperature and pressure (i.e., 60 °C and 1.2 MPa CO_2), compared to 4-week carbonation at atmospheric conditions (22 °C, fixed humidity 80, 5% CO_2 at atmosphere pressure). This would help to reduce the costs of the carbonation curing process.

References

1. Azdarpour A, Asadullah M, Mohammadian E, Hamidi H, Junin R, Karaei MA (2015) A review on carbon dioxide mineral carbonation through pH-swing process. Chem Eng J 279:615–630. doi:10.1016/j.cej.2015.05.064
2. Said A, Mattila HP, Jarvinen M, Zevenhoven R (2013) Production of precipitated calcium carbonate (PCC) from steelmaking slag for fixation of CO_2. Appl Energy 112:765–771. doi:10.1016/j.apenergy.2012.12.042
3. Pérez-Moreno S, Gázquez M, Bolívar J (2015) CO_2 sequestration by indirect carbonation of artificial gypsum generated in the manufacture of titanium dioxide pigments. Chem Eng J 262:737–746
4. Seifritz W (1990) CO_2 disposal by means of silicates. Nature 345(6275):486
5. Bobicki ER, Liu Q, Xu Z, Zeng H (2012) Carbon capture and storage using alkaline industrial wastes. Prog Energy Combust Sci 38(2):302–320. doi:10.1016/j.pecs.2011.11.002
6. Lackner KS (2003) A guide to CO_2 sequestration. Science 300(5626):1677–1678
7. Li W, Li B, Bai Z (2009) Electrolysis and heat pretreatment methods to promote CO_2 sequestration by mineral carbonation. Chem Eng Res Des 87(2):210–215. doi:10.1016/j.cherd.2008.08.001
8. Maroto-Valer MM, Fauth DJ, Kuchta ME, Zhang Y, Andrésen JM (2005) Activation of magnesium rich minerals as carbonation feedstock materials for CO_2 sequestration. Fuel Process Technol 86(14–15):1627–1645. doi:10.1016/j.fuproc.2005.01.017
9. Rao A, Anthony EJ, Manovic V (2008) Sonochemical treatment of FBC ash: a study of the reaction mechanism and performance of synthetic sorbents. Fuel 87(10–11):1927–1933. doi:10.1016/j.fuel.2007.11.007
10. Chang EE, Chen T-L, Pan S-Y, Chen Y-H, Chiang P-C (2013) Kinetic modeling on CO_2 capture using basic oxygen furnace slag coupled with cold-rolling wastewater in a rotating packed bed. J Hazard Mater 260:937–946. doi:10.1016/j.jhazmat.2013.06.052
11. Chang EE, Chiu A-C, Pan S-Y, Chen Y-H, Tan C-S, Chiang P-C (2013) Carbonation of basic oxygen furnace slag with metalworking wastewater in a slurry reactor. Int J Greenhouse Gas Control 12:382–389. doi:10.1016/j.ijggc.2012.11.026
12. Druckenmiller ML, Maroto-Valer MM (2005) Carbon sequestration using brine of adjusted pH to form mineral carbonates. Fuel Process Technol 86(14–15):1599–1614. doi:10.1016/j.fuproc.2005.01.007
13. Pan SY, Chiang PC, Chen YH, Tan CS, Chang EE (2013) Ex Situ CO_2 capture by carbonation of steelmaking slag coupled with metalworking wastewater in a rotating packed bed. Environ Sci Technol 47(7):3308–3315. doi:10.1021/es304975y
14. Pan S-Y, Chiang P-C, Chen Y-H, Tan C-S, Chang EE (2014) Kinetics of carbonation reaction of basic oxygen furnace slags in a rotating packed bed using the surface coverage model: maximization of carbonation conversion. Appl Energy 113:267–276. doi:10.1016/j.apenergy.2013.07.035
15. Santos RM, Ceulemans P, Van Gerven T (2012) Synthesis of pure aragonite by sonochemical mineral carbonation. Chem Eng Res Des 90(6):715–725. doi:10.1016/j.cherd.2011.11.022
16. Santos RM, François D, Mertens G, Elsen J, Van Gerven T (2013) Ultrasound-intensified mineral carbonation. Appl Therm Eng 57(1–2):154–163. doi:10.1016/j.applthermaleng.2012.03.035

17. Santos RM, Chiang YW, Elsen J, Van Gerven T (2014) Distinguishing between carbonate and non-carbonate precipitates from the carbonation of calcium-containing organic acid leachates. Hydrometallurgy 147–148:90–94. doi:10.1016/j.hydromet.2014.05.001
18. Jo H, Park S-H, Jang Y-N, Chae S-C, Lee P-K, Jo HY (2014) Metal extraction and indirect mineral carbonation of waste cement material using ammonium salt solutions. Chem Eng J 254:313–323. doi:10.1016/j.cej.2014.05.129
19. Dri M, Sanna A, Maroto-Valer MM (2013) Dissolution of steel slag and recycled concrete aggregate in ammonium bisulphate for CO_2 mineral carbonation. Fuel Process Technol 113:114–122. doi:10.1016/j.fuproc.2013.03.034
20. Kakizawa M, Yamasaki A, Yanagisawa Y (2001) A new CO_2 disposal process via artificial weathering of calcium silicate accelerated by acetic acid. Energy 26:341–354
21. Sun Y, Yao MS, Zhang JP, Yang G (2011) Indirect CO_2 mineral sequestration by steelmaking slag with NH4Cl as leaching solution. Chem Eng J 173:437–445
22. Eloneva S, Teir S, Salminen J, Fogelholm CJ, Zevenhoven R (2008) Fixation of CO_2 by carbonating calcium derived from blast furnace slag. Energy 33(9):1461–1467
23. Eloneva S, Puheloinen EM, Kanerva J, Ekroos A, Zevenhoven R, Fogelholm CJ (2010) Co-utilisation of CO_2 and steelmaking slags for production of pure $CaCO_3$-legislative issues. J Clean Prod 18:1833–1839
24. Teir S, Eloneva S, Fogelholm C-J, Zevenhoven R (2007) Dissolution of steelmaking slags in acetic acid for precipitated calcium carbonate production. Energy 32(4):528–539. doi:10.1016/j.energy.2006.06.023
25. Kodama S, Nishimoto T, Yamamoto N, Yogo K, Yamada K (2008) Development of a new pH-swing CO_2 mineralization process with a recyclable reaction solution. Energy 33(5): 776–784. doi:10.1016/j.energy.2008.01.005
26. Park A, Fan L (2004) mineral sequestration: physically activated dissolution of serpentine and pH swing process. Chem Eng Sci 59(22–23):5241–5247. doi:10.1016/j.ces.2004.09.008
27. New Energy and Industrial Technology Development Organization (NEDO) (1993) A survey on the current state of research and development for techniques to recover and sequester CO_2 from thermal power plants (II) (Karyoku hatsuden puranto karano CO_2 kaishu sisutemu ni kansuru chosa (II)) The Institute of Applied Energy (IAE). NEDO, Tokyo
28. Sanna A, Uibu M, Caramanna G, Kuusik R, Maroto-Valer MM (2014) A review of mineral carbonation technologies to sequester CO_2. Chem Soc Rev 43(23):8049–8080. doi:10.1039/c4cs00035h
29. Jung S, Wang LP, Dodbiba G, Fujita T (2014) Two-step accelerated mineral carbonation and decomposition analysis for the reduction of CO(2) emission in the eco-industrial parks. J Environ Sci (China) 26(7):1411–1422. doi:10.1016/j.jes.2014.05.006
30. Nduagu E, Bjorklof T, Fagerlund J, Makila E, Salonen J, Geerlings H, Zevenhoven R (2012) Production of magnesium hydroxide from magnesium silicate for the purposes of CO_2 minralization—Part 2: Mg extraction modeling and applcation to different Mg silicate rocks. Miner Eng 30(1):87–94
31. Costa G, Baciocchi R, Polettini A, Pomi R, Hills CD, Carey PJ (2007) Current status and perspectives of accelerated carbonation processes on municipal waste combustion residues. Environ Monit Assess 135(1–3):55–75. doi:10.1007/s10661-007-9704-4
32. Huntzinger DN, Gierke JS, Kawatra SK, Eisele TC, Sutter LL (2009) Carbon dioxide sequestration in cement kiln dust through mineral carbonation. Environ Sci Technol 43(6):1986–1992
33. Haug TA, Kleiv RA, Munz IA (2010) Investigating dissolution of mechanically activated olivine for carbonation purposes. Appl Geochem 25(10):1547–1563. doi:10.1016/j.apgeochem.2010.08.005
34. Pan S-Y, Chang EE, Chiang P-C (2012) CO_2 capture by accelerated carbonation of alkaline wastes: a review on its principles and applications. Aerosol Air Qual Res 12:770–791. doi:10.4209/aaqr.2012.06.0149

35. Chang EE, Pan S-Y, Chen Y-H, Chu H-W, Wang C-F, Chiang P-C (2011) CO_2 sequestration by carbonation of steelmaking slags in an autoclave reactor. J Hazard Mater 195:107–114. doi:10.1016/j.jhazmat.2011.08.006
36. Alper E, Wichtendahl B, Deckwer WD (1980) Gas absorption mechanism in catalytic slurry reactor. Chem Eng Sci 35:217–222
37. Ostergaard K (1968) Gas-liquid-particle operations in chemical reaction engineering. Adv Chem Eng 7:71–137. doi:10.1016/s0065-2377(08)60081-2
38. Chang EE, Chen CH, Chen YH, Pan SY, Chiang PC (2011) Performance evaluation for carbonation of steel-making slags in a slurry reactor. J Hazard Mater 186(1):558–564. doi:10.1016/j.jhazmat.2010.11.038
39. Monkman S, Shao Y, Shi C (2009) Carbonated ladle slag fines for carbon uptake and sand substitute. J Mater Civ Eng 21:657–665. doi:10.1061//asce/0899-1561/2009/21:11/657
40. Chang EE, Pan SY, Yang L, Chen YH, Kim H, Chiang PC (2015) Accelerated carbonation using municipal solid waste incinerator bottom ash and cold-rolling wastewater: performance evaluation and reaction kinetics. Waste Manag 43:283–292. doi:10.1016/j.wasman.2015.05.001
41. Lin C, Chen B (2008) Characteristics of cross-flow rotating packed beds. J Ind Eng Chem 14 (3):322–327. doi:10.1016/j.jiec.2008.01.004
42. Wang M (2004) Controlling factors and mechanism of preparing needlelike $CaCO_3$ under high-gravity environment. Powder Technol 142(2–3):166–174. doi:10.1016/j.powtec.2004.05.003
43. Kelleher T, Fair JR (1996) Distillation studies in a high-gravity contactor. Ind Eng Chem Res 35:4646–4655
44. Yu C-H, Huang C-H, Tan C-S (2012) A review of co_2 capture by absorption and adsorption. Aerosol Air Qual Res 12:745–769. doi:10.4209/aaqr.2012.05.0132
45. Chen YH, Huang YH, Lin RH, Shang NC (2010) A continuous-flow biodiesel production process using a rotating packed bed. Bioresour Technol 101(2):668–673. doi:10.1016/j.biortech.2009.08.081
46. Chen YH, Chang CY, Su WL, Chen CC, Chiu CY, Yu YH, Chiang PC, Chiang SIM (2004) Modeling ozone contacting process in a rotating packed bed. Ind Eng Chem Res 43(1): 228–236
47. Cheng H-H, Tan C-S (2011) Removal of CO_2 from indoor air by alkanolamine in a rotating packed bed. Sep Purif Technol 82:156–166. doi:10.1016/j.seppur.2011.09.004
48. Pan SY, Chiang PC, Chen YH, Chen CD, Lin HY, Chang EE (2013) Systematic approach to determination of maximum achievable capture capacity via leaching and carbonation processes for alkaline steelmaking wastes in a rotating packed bed. Environ Sci Technol 47(23):13677–13685. doi:10.1021/es403323x
49. Chang EE, Pan SY, Chen YH, Tan CS, Chiang PC (2012) Accelerated carbonation of steelmaking slags in a high-gravity rotating packed bed. J Hazard Mater 227–228:97–106. doi:10.1016/j.jhazmat.2012.05.021
50. Pan SY, Chen YH, Chen CD, Shen AL, Lin M, Chiang PC (2015) High-gravity carbonation process for enhancing CO_2 fixation and utilization exemplified by the steelmaking industry. Environ Sci Technol 49(20):12380–12387. doi:10.1021/acs.est.5b02210
51. Rao A, Anthony EJ, Jia L, Macchi A (2007) Carbonation of FBC ash by sonochemical treatment. Fuel 86(16):2603–2615. doi:10.1016/j.fuel.2007.02.004
52. Huang C-H, Tan C-S (2014) A review: CO_2 utilization. Aerosol Air Qual Res 14:480–499. doi:10.4209/aaqr.2013.10.0326
53. McCutcheon J, Power IM, Harrison AL, Dipple GM, Southam G (2014) A greenhouse-scale photosynthetic microbial bioreactor for carbon sequestration in magnesium carbonate minerals. Environ Sci Technol 48(16):9142–9151. doi:10.1021/es500344s
54. Miyamoto K (2009) Biological energy production. In: Renewable biological systems for alternative sustainable energy production (FAO Agricultural Services Bulletin - 128). Food and Agriculture Organization of the United Nations

55. Lindskog S (1997) Structure and mechanism of carbonic anhydrase. Pharmacol Ther 74(1): 1–20
56. Li W, Chen W-S, Zhou P-P, Zhu S-L, Yu L-J (2013) Influence of initial calcium ion concentration on the precipitation and crystal morphology of calcium carbonate induced by bacterial carbonic anhydrase. Chem Eng J 218:65–72. doi:10.1016/j.cej.2012.12.034
57. Li W, Chen W-S, Zhou P-P, Yu L-J (2013) Influence of enzyme concentration on bio-sequestration of CO_2 in carbonate form using bacterial carbonic anhydrase. Chem Eng J 232:149–156. doi:10.1016/j.cej.2013.07.069
58. Figueroa JD, Fout T, Plasynski S, McIlvried H, Srivastava RD (2008) Advances in CO_2 capture technology—The U.S. Department of Energy's carbon sequestration program. Int J Greenhouse Gas Control 2(1):9–20. doi:10.1016/s1750-5836(07)00094-1
59. Uibu M, Kuusik R (2009) Mineral trapping of CO_2 via oil shale ash aqueous carbonation: controlling mechanism of process rate and development of continuous-flow reactor system. Oil Shale 26(1):40. doi:10.3176/oil.2009.1.06
60. Liu Q, Mercedes Maroto-Valer M (2011) Investigation of the effect of brine composition and pH buffer on CO_2-brine sequestration. Energy Procedia 4:4503–4507. doi:10.1016/j.egypro.2011.02.406
61. Liu Q, Maroto-Valer MM (2012) Studies of pH buffer systems to promote carbonate formation for CO_2 sequestration in brines. Fuel Process Technol 98:6–13. doi:10.1016/j.fuproc.2012.01.023
62. Brady PV (1996) Physics and chemistry of mineral surfces. Chemistry and physics of surfaces and minerals. CRC Press LLC, Florida
63. Hangx SJT (2005) Behaviour of the CO_2-H_2O system and preliminary mineralisation model and experiments. Subfurface mineralisation: rate of CO_2 mineralisation and geomechanical effects on host and seal formations. Shell International Exploration and Production (leader CATO WP 4.1)
64. Krevor SCM, Lackner KS (2011) Enhancing serpentine dissolution kinetics for mineral carbon dioxide sequestration. Int J Greenhouse Gas Control 5(4):1073–1080. doi:10.1016/j.ijggc.2011.01.006
65. O' Connor WK, Dahlin DC, Rush GE, Gerdemann SJ, Penner LR, Nilsen DN (2005) Aqueous mineral carbonation: Mineral availability, pretreatment, reaction parameters, and process studies. Albany Research Center (ARC), U.S.A
66. Beard JS, Blencoe JG, Anovitz LM, Palmer DA (2004) Carbonation of metal silicates for long-term CO_2 sequestration. Canada Patent
67. Jo H, Jang Y-N, Young Jo H (2012) Influence of NaCl on mineral carbonation of CO_2 using cement material in aqueous solutions. Chem Eng Sci 80:232–241. doi:10.1016/j.ces.2012.06.034
68. Nyambura MG, Mugera GW, Felicia PL, Gathura NP (2011) Carbonation of brine impacted fractionated coal fly ash: implications for CO_2 sequestration. J Environ Manage 92(3):655–664. doi:10.1016/j.jenvman.2010.10.008
69. El-Hassan H, Shao Y (2015) Early carbonation curing of concrete masonry units with Portland limestone cement. Cement Concr Compos 62:168–177. doi:10.1016/j.cemconcomp.2015.07.004
70. Borges PHR, Costa JO, Milestone NB, Lynsdale CJ, Streatfield RE (2010) Carbonation of CH and C-S–H in composite cement pastes containing high amounts of BFS. Cem Concr Res 40:284–292. doi:10.1016/j.cemconres.2009.10.020
71. Zhang F, Mo L, Deng M (2015) Mechanical strength and microstructure of mortars prepared with MgO-CaO-Fly ash-Portland cement blends after accelerated carbonation. J Chin Ceram Soc 43(8):1–8. doi:10.14062/j.issn.0454-5648.2015.08.01
72. Ghouleh Z, Guthrie RIL, Shao Y (2015) High-strength KOBM steel slag binder activated by carbonation. Constr Build Mater 99:175–183. doi:10.1016/j.conbuildmat.2015.09.028
73. Mo L, Zhang F, Deng M (2015) Effects of carbonation treatment on the properties of hydrated fly ash-MgO-Portland cement blends. Constr Build Mater 96:147–154. doi:10.1016/j.conbuildmat.2015.07.193

74. Wu HZ, Chang J, Pan ZZ, Cheng X (2009) Carbonate steelmaking slag to manufacture building materials. Adv Mater Res 79–82:1943–1946. doi:10.4028/www.scientific.net/AMR.79-82.1943
75. Wu HZ, Chang J, Pan ZZ, Cheng X (2011) Effects of carbonation on steel slag products. Adv Mater Res 177:485–488. doi:10.4028/www.scientific.net/AMR.177.485
76. Liang XJ, Ye ZM, Chang J (2012) Early hydration activity of composite with carbonated steel slag. J Chin Ceram Soc 40(2):228–233 (in Chinese)
77. Salman M, Cizer Ö, Pontikes Y, Santos RM, Snellings R, Vandewalle L, Blanpain B, Van Balen K (2014) Effect of accelerated carbonation on AOD stainless steel slag for its valorisation as a CO_2-sequestering construction material. Chem Eng J 246:39–52. doi:10.1016/j.cej.2014.02.051
78. Salman M, Cizer Ö, Pontikes Y, vandewalle L, blanpain B, Van Balen K (2013) Carbonation potential of continuous casting stainless steel slag. Paper presented at the Acelerated Carbonation for Environmental and Material Engineering KU Leuven, Belgium